

1 **Proteomic network analysis of bronchoalveolar lavage fluid in ex-smokers to discover**
2 **implicated protein targets and novel drug treatments for chronic obstructive pulmonary**
3 **disease**

4 Manoj J. Mammen^{1,6}, Chengjian Tu^{2,3}, Matthew C. Morris⁵, Spencer Richman⁵, William
5 Mangione⁶, Zackary Falls⁶, Jun Qu^{2,3}, Gordon Broderick⁵, Sanjay Sethi^{1,4}, Ram Samudrala⁶

6

7 ¹Department of Medicine, Jacobs School of Medicine and Biological Sciences, State University
8 of New York at Buffalo, Buffalo, NY 14214 USA; ²Department of Pharmaceutical Sciences,
9 State University of New York at Buffalo, Buffalo, NY 14260 USA; ³New York State Center of
10 Excellence in Bioinformatics and Life Sciences, 701 Ellicott Street, Buffalo, NY 14203 USA;
11 ⁴WNY VA Healthcare System, Buffalo, NY 14215 USA; ⁵Center for Clinical Systems Biology,
12 Rochester General Hospital, Rochester, NY 14621 USA; Department of Biomedical Informatics,
13 Jacobs School of Medicine and Biological Sciences, State University of New York, Buffalo, NY
14 14214 USA; ⁶Department of Biomedical Informatics, Jacobs School of Medicine and Biological
15 Sciences, State University of New York, Buffalo, NY 14214 USA

16

17 ***Corresponding Authors:**

18 Manoj J. Mammen, MD, MS

19 100 High Street, B-8

20 Buffalo, NY 14203

21 Phone: (716) 859-2271

22 Email: mammen@buffalo.edu

23 Ram Samudrala, PhD

24 77 Goodell St.

25 Buffalo, NY 14203

26 Phone: (206) 251-8852

27 Email: rams@buffalo.edu

28 **Authors and Contributors:** MJM, CT, JQ, MCM, WM, ZF, SR, GB, SS, RS

29 **Funding Sources:** Dr. Mammen was supported by a research grant from the University at
30 Buffalo. A National Heart, Lung and Blood Institute grant to Dr. Sethi supported the collection
31 of Bronchoalveolar lavage specimens. This work is also supported, in part, by National Institute
32 Health (NIH) awards U54HD071594 (JQ) and by American Heart Association (AHA) award
33 12SDG9450036 (JQ). Rochester Regional Health also supported this work in conjunction with
34 the US Department of Defense Congressionally Directed Medical Research Programs (CDMRP)
35 under the Peer Reviewed Medical Research Program (PRMRP) award W81XWH1910804
36 (Broderick - PI; Sethi - Partnering PI, JQ-CoI), as well as by Elsevier AB (Amsterdam). The
37 development of the CANDO platform was supported in part by a NIH Director's Pioneer Award
38 (DP1OD006779), NIH Clinical and Translational Sciences Award (UL1TR001412), NIH
39 Buffalo Research Innovation in Genomic and Healthcare Technology Education Award
40 (T15LM012495), NIH NCATS ASPIRE Design Challenge Award, NIH NCATS ASPIRE
41 Reduction-to-Practice Award, and startup funds from the Department of Biomedical Informatics
42 at the University at Buffalo.

43

44 **MANDATORY DISCLAIMER**

45 The opinions and assertions contained herein are the private views of the authors and are not to
46 be construed as official or as reflecting the views of the Department of Defense.

47

48 To obtain the raw proteomic data on a DVD media, please contact Dr. Jun Qu, junqu@buffalo.edu.

49

50 **Running title:** Computational analysis of BALF proteome to repurpose drugs for COPD.

51 **Word Count:**

52 **Keywords:** proteomics, drug repurposing, translational bioinformatics, interaction signature,

53 bronchoalveolar lavage fluid, chronic obstructive pulmonary disease, label-free quantitation,

54 plasma, serum, biomarker

55

56 **Abbreviations:** BALF=bronchoalveolar lavage fluid; BANDOCK= bioanalytical docking;

57 CANDO=computational analysis of novel drug opportunities; COPD= chronic obstructive

58 pulmonary disease; DAVID=database for annotation visualization and integrated discovery;

59 GO= gene ontology; IPA= ingenuity pathway analysis; LTQ Orbitrap=linear ion trap combined

60 with an orbitrap analyzer mass spectrometer.

61

62

63 **Abstract**

64 **Rationale:** Bronchoalveolar lavage of the epithelial lining fluid can sample the profound
65 changes in the airway lumen milieu prevalent in Chronic Obstructive Pulmonary Disease
66 (COPD). Characterizing the proteins in bronchoalveolar lavage fluid in COPD with advanced
67 proteomic methods will identify disease-related changes, provide insight into pathogenetic
68 mechanisms and potential therapeutics that will aid in the discovery of more effective
69 therapeutics for COPD.

70

71 **Objectives:** We compared epithelial lining fluid proteome of ex-smokers with moderate COPD
72 who are not in exacerbation status COPD, to non-smoking healthy control subjects using
73 advanced proteomics methods and applied proteome-scale translational bioinformatics
74 approaches to identify potential therapeutic protein targets and drugs that modulate these proteins
75 towards the treatment of COPD.

76

77 **Methods:** Proteomic profiles of bronchialveolar lavage fluid were obtained from 1) never-smoker
78 control subjects with normal lung function (n=10) or 2) individuals with stable moderate (GOLD
79 stage 2, FEV₁ 50% – 80% predicted) COPD who were ex-smokers for at least one year (n=10).
80 NIH's Database for Annotation, Visualization and Integrated Discovery (DAVID) and
81 Ingenuity's Ingenuity Pathway Analysis (IPA) were the two bioinformatics tools employed for
82 network analysis on the differentially expressed proteins to identify potential crucial hub
83 proteins. The drug-proteome interaction signature comparison and ranking approach
84 implemented in the Computational Analysis of Novel Drug Opportunities (CANDO) platform
85 for multiscale therapeutic discovery was utilized to identify potential repurposable drugs for the

86 treatment of COPD based on the BALF proteome. Subsequently, a literature-based knowledge
87 graph was utilized to rank combinations of drugs that would most likely ameliorate inflammatory
88 processes by inhibition or activation of their functions.

89

90 **Results:** Proteomic network analysis demonstrated that 233 of the >1800 proteins identified in
91 the BALF were differentially expressed in COPD versus control, including proteins associated
92 with inflammation, structural elements, and energy metabolism. Functional annotation of the
93 differentially expressed proteins by their implicated biological processes, cellular localization,
94 and transcription factor interactions was accomplished via DAVID. Canonical pathways
95 containing the differential expressed proteins were detailed via the Ingenuity Pathway Analysis
96 application. Topological network analysis demonstrated that four proteins act as central node
97 proteins in the inflammatory pathways in COPD. The CANDO multiscale drug discovery
98 platform was used to analyze the behavioral similarity between the interaction signatures of all
99 FDA-approved drugs and the identified BALF proteins. The drugs with the signatures most
100 similar interaction signatures to approved COPD drugs were extracted with the CANDO
101 platform. The analysis revealed 189 drugs that putatively target the proteins implicated in
102 COPD. The putative COPD drugs that were identified using CANDO were subsequently
103 analyzed using a knowledge based technique to identify an optimal two drug combination that
104 had the most appropriate effect on the central node proteins.

105

106 **Conclusion:** Analysis of the BALF proteome revealed novel differentially expressed proteins in
107 the epithelial lining fluid that elucidate COPD pathogenesis. Network analyses identified critical
108 targets that have critical roles in modulating COPD pathogenesis, for which we identified several

109 drugs that could be repurposed to treat COPD using a multiscale shotgun drug discovery

110 approach.

111

112

113 **Introduction**

114 Chronic obstructive pulmonary disease (COPD) is a leading cause of mortality and morbidity in
115 the US.¹⁻⁵ Additionally, COPD results in millions of hospitalizations in the developing world.^{1,6-}

116 ¹¹ The prevalence of cigarette smoking continues to rise in most developing countries around the
117 world.¹²⁻¹⁴ However, only 25-50% of tobacco smokers develop COPD, suggesting only a subset

118 develops an exaggerated inflammatory process that leads to lung destruction.^{12,13,15}

119 Bronchoalveolar lavage fluid (BALF) and bronchial samples from ex-smokers reveal active
120 inflammation long after smoking cessation.¹⁶

121

122 Although structural changes in the airways, parenchyma, and pulmonary vessels are typical in
123 patients with COPD, the lower airways and the alveoli are the initial sites of the inflammatory
124 process.^{17,18} The inflammatory process initiated by smoking persists after cessation and is likely
125 exaggerated by autoimmunity and infection.^{19,20} Accurate and precise measurement of the
126 molecular mediators in the airways should aid in rigorous analysis of their role in disease.

127

128 There has been a keen interest in understanding the genetic determinants of COPD, as the
129 interaction between genes and environment leads to protein expression, ultimately resulting in
130 either healthy or disease states. However, genomic data alone does not predict protein abundance
131 or activity; proteins are the ultimate participants in integrated biological processes that lead to
132 healthy physiological function or pathology. Proteome-based analysis of bronchoalveolar lavage

133 fluid (BALF) in COPD can identify tissue-specific markers of inflammation that can lead to
134 understanding the mechanisms of COPD progression.

135

136 We sought to determine an unbiased proteome-based analysis of BALF in COPD under stable
137 conditions (not in exacerbation status) to identify a broad series of molecules involved in COPD
138 pathogenesis. A label-free proteomics mass spectroscopy method was utilized. The differentially
139 expressed proteins were analyzed using multiple bioinformatics tools to critical pathways that
140 were altered in these ex-smoker patients with COPD compared to healthy, never smoker
141 controls, proteins implicated in COPD etiology, and to identify putative drug candidates that can
142 be repurposed to treat COPD.

143

144 The raw proteomic data used in this manuscript was initially detailed in a previously published
145 methodology manuscript using strict criteria (2 peptide identification criteria for a protein, ≥ 1.5
146 fold change, and $p\text{-value} < 0.05$) to identify 423 individual proteins with 76 proteins expressed
147 differently between COPD and controls.²¹ In this analysis, we adopted a pragmatic approach to
148 the same raw proteomic data (1 peptide identification criterion, ≥ 1.5 fold change, and $p\text{-}$
149 $p\text{-value} < 0.05$) that identified 1831 individual proteins and 233 differentially expressed proteins
150 between the two groups. The latter, more practical, approach provides important additional
151 information for biomarker and therapeutic target discovery that may be utilized in future research
152 to discover useful interventions.

153 **Methods**

154

155 We analyzed the protein quantifications derived from the BALF of subjects with COPD and
156 healthy ex-smoker control subjects via liquid chromatography and mass spectroscopy. We then
157 used pathway analysis tools to identify relevant cellular pathways associated with differentially
158 expressed proteins quantified from the BALF analysis. We subsequently employed the
159 Computational Analysis of Novel Drug Opportunities (CANDO) platform to identify FDA
160 approved drugs that could be repurposed to COPD, based on their putative interaction with the
161 differentially expressed proteins. Using topological network analysis, we identified putative hub
162 proteins that modulate the cellular pathways associated with COPD. Using the medical literature
163 to predict the repurposed drugs effects on the most important hub protein, we created a refined
164 list of drugs predicted to modulate the cellular pathway in order to impede COPD pathogenesis.
165 to generate proteomic interaction signatures for the compounds

166

167 **Recruitment of subjects**

168 BALF was obtained in a NHLBI funded study of innate lung defense in COPD.²² All procedures
169 received approval from the Institutional Review Board (IRB), Veterans Affairs Western New
170 York Healthcare System (WNY-VA), and strictly adhered to institutional guidelines.

171

172 **Ethics statement**

173
174 This study is a sub-study of a larger group of patients with COPD and healthy controls to
175 understand biological determinants of exacerbation frequency and was approved by the
176 Institutional Review Boards of the Veterans Affairs Western New York Healthcare System and

177 University at Buffalo. The participants gave written consent to the study via an IRB-approved
178 consent form.

179

180 **Inclusion/exclusion criteria**

181
182 The inclusion criteria and procedures for this study have been described previously and are
183 provided in the supplementary material.²² After informed consent, 116 volunteers were divided
184 into three groups: 1) healthy nonsmokers, 2) ex-smokers with COPD, and 3) active smokers with
185 COPD and underwent bronchoscopy and bronchoalveolar lavage. The methodology for
186 bronchoscopy, lavage, and sample processing is included in the supplementary material.

187

188 For this study, we selected BALF obtained from ten ex-smokers with moderate COPD and ten
189 healthy non-smoking controls for proteomic analysis, respectively. To minimize variability due
190 to effects of acute smoking and disease severity, we confined this analysis to ex-smokers and
191 moderate stage 2 disease per the Global Obstructive Lung Disease (GOLD)²³ criteria of the

192 forced expiratory volume in 1 second (FEV₁) 50-80% predicted. All ex-smokers had ceased
193 smoking for at least one year.

194

195 **Bronchoscopy and BALF sample preparation**

196 The research bronchoscopy and BALF sample preparation were performed as described
197 previously.²⁴

198

199 **Protein identification/quantification.**

200 To investigate the soluble molecules in the epithelial lining fluid that may participate in COPD
201 pathogenesis, unbiased proteomic analysis of BALF commenced without protein depletion or
202 fractionation. Details of the methodology have been published²⁵ and are also provided in the
203 supplementary material.

204

205 **Long gradient nano-RPLC/mass spectrometry**

206 Complete separation of the complex peptide mixture utilized a nano-LC/nanospray setup;²⁶ the
207 ion-current long gradient approach with mass spectrometry and subsequent protein identification
208 was performed as described in Tu, et al. ²⁵⁻²⁷ All proteins identified with one or more peptide
209 hits, fold change of ≥ 1.5 , and p-value < 0.05 are included as part of the differentially expressed
210 BALF proteome.

211

212 **Bioinformatics analyses**

213 *Manually curated pathway analysis*

214 Gene ontology, transcription factors, and expression locations were determined by uploading the

215 protein expression dataset onto a web-based tool, the NIH's Database for Annotation,

216 Visualization and Integrated Discovery (DAVID) v6.7 (<http://david.abcc.ncifcrf.gov/>).^{28,29}

217 Biological networks were generated with Ingenuity Pathway Analysis (IPA, Ingenuity Systems),

218 a web-based relational database and network generator. Proteins overrepresented in the uploaded

219 datasets in biological networks, canonical pathways, and biological processes were identified.

220

221 *Literature informed protein-protein and protein-drug interaction network*

222 In addition to annotating differentially expressed proteins with the manually curated pathways

223 cataloged in IPA, a network of protein-protein interactions was created using known regulatory

224 relationships extracted from published scientific literature using the MedScan text-mining

225 engine³⁰ as well as protein-drug interactions cataloged in the Reaxsys medicinal chemistry

226 database (Elsevier, Amsterdam). These are embedded in the broader Elsevier Knowledge Graph

227 database³¹ and were accessed via the Pathway Studio interface (Elsevier, Amsterdam).³²

228

229 *Shotgun multiscale drug discovery platform*

230 We used the Computational Analysis of Novel Drug Opportunities (CANDO) platform³³⁻⁴⁰ to

231 predict drugs that can be repurposed for the treatment of stable COPD. In CANDO, a

232 compound/drug is considered to be potentially repurposable for an indication when it is found to

233 have similar binding interactions with a specific proteome or library of proteins as a drug with
234 known approval for the indication of interest.

235

236 In this study, we calculated the interaction scores between 2,450 United States Federal Drug
237 Administration (FDA) approved drugs from the CANDO version 2.3 compound library and a
238 curated human library of 8,385 proteins, including 5,316 solved X-ray crystallography structures
239 and 3,069 computed protein structures modeled by I-TASSER^{41,42}. The interaction scores were
240 calculated using the bioanalytic docking (BANDOCK) protocol in the CANDO which utilizes
241 predicted binding site information and chemical similarity to determine an interaction score that
242 is a surrogate for the likelihood of interaction between a compound and protein.³³ Binding sites
243 were predicted for all human proteins using COACH⁴³, which uses the consensus of three
244 complementary methods utilizing structure and sequence information to find similarity to solved
245 structures in the Protein Data Bank (PDB).^{44,45} For each binding site predicted by COACH, a
246 confidence score (PScore) and an associated co-crystallized ligand are output. The ligand is then
247 compared to the query compound/drug using chemical fingerprinting methods, which
248 enumerates the presence or absence of molecular substructures on the compound/drug. The
249 Sorenson-Dice coefficient⁴⁶ between the protein-ligand and compound/drug fingerprints
250 (CScore) is also computed. The BANDOCK interaction score outputted for each compound-
251 protein pair is the product of the Pscore and the Cscore.

252

253 For this analysis, we focused on the differentially expressed proteins in the BALF proteome (as
254 described), and drugs used to treat COPD ("MESH:D029424") (Table S1). We selected proteins
255 in the CANDO human protein library that were also represented in the differentially expressed

256 BALF proteome. We then used the CANDO platform to predict the top drug candidates that
257 could be repurposed to treat COPD based on compound-proteome interaction signature
258 similarity to drugs currently approved/used to treat stable COPD. The protocol iterates through
259 34 known drugs used to treat stable COPD, counting the number of times drugs not associated
260 with COPD show up in the top30 most similar compounds to the known treatments, then outputs
261 the consensus predictions ranked by the number of times each compound appeared across all
262 top30 lists. The similarity between a given drug and all other drugs in the library is determined
263 by comparing their proteomic interaction signatures using the cosine similarity metric, where
264 compounds with greater similarity scores rank stronger than those with low similarity. Thereby
265 drugs that were most similar (in terms of interaction signatures) to multiple drugs used to treat
266 COPD will be ranked highest.

267
268 *Network topological analysis*
269 Although not a complete descriptor, the topological location, and aspects of the connectivity
270 linking a node to a broader biological network can inform the node's function in mediating
271 network behavior. Among the measures of a node's importance or centrality, *betweenness*
272 centrality has been used to describe how a node might serve as an important mediator of
273 information flow in a regulatory network. In this work, $C_b(n)$ for each node n of a network was
274 calculated using the Brandes algorithm.⁴⁷ The betweenness centrality of a node n reflects the

275 amount of control that this node exerts over the interaction between communities of neighboring
276 nodes in the network⁴⁸ and can be computed as follows:

277

$$C_b(n) = \sum_{s \neq t \neq n} \left(\frac{\sigma_{s,t}(n)}{\sigma_{s,t}} \right) \quad (1)$$

278 Where s and t are the source and target nodes in the network different from n , $\sigma_{s,t}$ denotes the
279 number of shortest paths from all s to all t , and $\sigma_{s,t}(n)$ is the number of shortest paths from s to t
280 that must pass through node n . Here, unweighted betweenness centralities were calculated for
281 each node in the literature-informed protein-protein network. The betweenness centrality scores
282 for all nodes were expressed as fractions of the maximum betweenness centrality present in the
283 network. All calculations were conducted in R version 4.0.2.⁴⁹

284

285 Literature based drug enrichment analysis

286 Using putative drugs ranked by CANDO and further analyzed via the Elsevier Knowledge
287 Graph,³¹ a drug enrichment analysis was performed to predict which drugs can most closely mimic
288 an idealized intervention against the hub proteins identified in the network topological analysis.
289 Drugs are represented as vectors with a length equal to the empirically derived number protein
290 entities in the network model. Each index value is listed as 0 if there is no interaction between the
291 drug and the corresponding model entity, a 1 if the drug promotes that entity, or a -1 if the drug
292 inhibits that entity. Next, the cosine similarity, S_c , between each drug vector and the idealized
293 intervention vector is calculated.⁵⁰ Cosine similarity is calculated as:

294

$$S_c(D, M) = \frac{D \cdot M}{\|D\| \|M\|}$$

295 Where D is the drug vector and M is the idealized intervention. Higher S_c indicates a closer match
296 between the drug vector and the idealized vector. A S_c of 1 means the two vectors are identical,

297 and -1 indicates that the two are exactly opposed. For multidrug combinations, the net-effect of
298 the individual drug vectors is calculated as:

299

$$sgn \left(\sum_{i=1}^n \vec{d}_i D_i \right)$$

300 Where n is the total number of drugs in the combination, D_i is the vector corresponding to the i th
301 drug, and sgn is the sign function. The cosine similarity of the net-effect vector and idealized vector
302 is then calculated.

303 The statistical significance of these enrichment scores is determined empirically from an
304 estimated null distribution of cosine similarities. This null distribution uses a set of model-relevant

305 background drugs for which each interacts with at least one entity in the network. All CANDO
306 drugs of interest were included in the background. Empirical p-values are estimated as

307
$$\hat{p} = \frac{(r + 1)}{(n + 1)}$$

308 Where r is the number of null S_c values greater than the observed S_c and n is the total number of
309 null S_c values.

310

311 **Statistical analysis**

312 Statistical analysis was performed with SPSS/19. Demographic values were depicted as mean \pm
313 SEM.

314

315 **Results**

316 ***Study population characteristics***

317 Characteristics for subjects included in the BALF study are shown in **Table 1**, with the only
318 significant differences between the two groups in tobacco smoke exposure and lung function.

319

320 ***BALF proteome characteristics***

321 A total of 1831 unique proteins were identified in the BALF proteome. A total of 233 proteins
322 (>1.5 -fold absolute change, p-value <0.05) had a significant differential expression in BALF
323 samples from patients with COPD versus healthy ex-smokers, 138 proteins were decreased in
324 COPD while 95 proteins were increased (**Table S2 and Table S3**).

325

326 ***Manually curated pathway analysis***

327 *Functional annotation of differential expressed proteins and transcription factor interactions*

328 The 233 differentially quantified proteins were characterized by their biological processes,
329 transcription factor interactions, and cellular localization by employing NIH's DAVID.^{28,29} The
330 proteins involved in several biological processes implicated in COPD pathogenesis (total number
331 of proteins, number upregulated, number downregulated) such as proteolysis⁵¹ (20,4,16),
332 extracellular matrix⁵² (13,6,7), cell adhesion⁵³ (11,2,9), cytoskeleton⁵⁴ (32,14,18), defense
333 response⁵⁵ (16, 7,9), cell migration⁵⁶ (12,4,8), and oxidation-reduction²¹ (11,2,9) were altered in
334 COPD. As expected with examining the lung lining fluid, the largest single group of
335 differentially expressed proteins was associated with the extracellular space (49, 30, 19).

336

337 Transcription factors (**Table S4**) associated with the differentially expressed proteins (total
338 number of proteins associated with the transcription factor) included serum response factor-SRF
339 (148), transcription factor 8-AREB6 (166), signal transducer and activator of transcription factor
340 1-STAT1 (69), zinc finger protein-GFI1 (97), signal transducer and activator of transcription
341 factor 3-STAT3 (101), nuclear factor kappa-light-chain-enhancer of activated B cells-NF- κ B
342 (79), CCAAT/enhancer-binding protein β -CEBPB(109), paired box gene 2-PAX2(113), and
343 activating transcription factor 2-CREBP1(95).

344

345 *Bioinformatic pathway analysis of BALF proteomic data*

346 The protein expression datasets were imported into IPA (Ingenuity Systems) and projected onto
347 the relevant biological pathways; processes linked to the differentially expressed proteins were
348 analyzed with IPA's manually curated knowledge database. Of the 233 differentially expressed
349 proteins, 217 matched to the IPA curated database and were analyzed. Sixteen pathways were
350 noted to have several proteins associated with the differentially expressed BALF dataset (**Table**

351 **S5**), including proteins implicated in cellular movement, cellular death and survival, cell
352 morphology, immune cell trafficking, and cell cycle. Appendix **Figures S1 to S4** depict IPA
353 networks of selected pathways with the highest number of differentially expressed proteins.

354

355 ***Computational drug prediction***

356 130 out of 233 BALF differentially expressed proteins were identified in the CANDO human
357 protein library. This subset of proteins within the CANDO platform was used to predict 189
358 putative drug candidates that have the most similar protein interaction signatures to the set of
359 known drugs used to treat COPD (**Figure 1** and **Table S6**). Many of the drugs were
360 corticosteroids; however other putative drugs included tezacaftor⁵⁷, a recently developed drug to
361 potentiate sodium channel activity in the treatment of cystic fibrosis; two additional drugs
362 predicted to treat COPD, gemfibrozil⁵⁸, and pioglitazone⁵⁹, are drugs currently used to treat
363 hyperlipidemia and diabetes, respectively.

364

365 ***Candidate key mediators of COPD pathology based on literature derived drug enrichment***

366 *Literature informed protein-protein and protein-drug interaction network*

367 A total of 233 proteins were identified as differentially expressed between COPD patients and
368 healthy controls by mass spectrometry. Of these, 214 were represented in the Elsevier
369 Knowledge Graph³¹, with the remainder comprising specific immunoglobulin chain proteins. A
370 query of the Knowledge Graph for documented regulatory interactions between these protein
371 entities yielded 206 regulatory edges supported by 807 references (with a median of 1 reference
372 per edge). 112 of the 214 identified proteins could not be connected to the broader network
373 circuit by a documented interaction. The protein entities in this network were then assessed in

374 terms of their importance as mediators of signal transfer based on their betweenness centrality.
375 (**Figure 2**).

376

377 Network topological analysis

378 Four nodes representing proteins in the network stood out based on the normalized betweenness
379 centrality values representing a greater than linear increase from the next lower ranking node:
380 fibronectin, vimentin, intercellular adhesion molecule 1 (ICAM1), and galectin-3. These
381 potentially key signaling mediators had a betweenness centrality of at least 25% of the
382 maximum.

383

384 Analysis of the initial data reveals fibronectin and ICAM1 are reduced in COPD patients relative
385 to healthy controls; thus, any candidate therapeutic should target an increase in their activity. The
386 reverse is true for vimentin and galectin-3. We, therefore, sought drugs or combinations of drugs
387 predicted to accomplish the appropriate activation or inhibition of the four most central nodes,
388 specifically drugs that will lead to the promotion of central node proteins that were
389 downregulated in the COPD cohort and inhibition of central node proteins that were
390 overabundant in COPD. The idealized drug vector, therefore, constitutes interactions leading to
391 desirable modulation of the central hub protein. CANDO identified 189 distinct drugs (**Figure**
392 **1, Table S7S6**) with relevance for COPD; 39 of these represented in the Elsevier Knowledge
393 Graph³¹ were analyzed for their enrichment for the desired agonist and antagonist effects on the
394 most central entities in the protein regulatory network. Highly enriched drugs or drug pairs were
395 are predicted to be more likely than randomly selected drugs to exert appropriate inhibition or
396 promotion of the most central proteins. Two single drugs (fluocinolone acetonide and

397 dexrazoxane) and 57 two-drug combinations were significantly enriched. Fluocinolone acetonide
398 and dexrazoxane appeared in 54% and 46% of all significantly enriched 2-drug combinations,
399 respectively, far greater than the other drugs appearing in these combinations (Figure 3). The
400 combination of fluocinolone acetonide and dexrazoxane is the most enriched two-drug
401 combination leading to an idealized drug vector.

402
403 We additionally conducted a targeted query to assess the predicted effects of drugs commonly
404 applied in pulmonary disease treatment on the most central proteins of this regulatory network
405 (Figure 4 and Table S7). While some of these have been documented to have the desired effect
406 on two of the central proteins, fibronectin or vimentin, all have been documented to have the
407 opposite effect on at least one of the most central proteins. Therefore, they were not significantly
408 enriched out of the set of all possible candidate drugs.

409

410 **Discussion**

411 Our investigation of the COPD BALF proteome utilizing novel bioinformatic techniques
412 revealed significant differences in proteins involved in multiple biological processes, including
413 lung-specific mechanisms, protease/anti-protease homeostasis, immunoregulation, and the
414 extracellular matrix. Proteomic profiling of the complex pathways implicated in COPD provides
415 broader physiological exploration not provided by studying one entity at a time. We identified
416 several differentially expressed proteins in COPD versus controls that, based on a review of
417 published literature, have not been previously implicated in COPD etiology. This preliminary
418 analysis illustrates how our BALF proteomic analysis represents a powerful approach to
419 elucidate COPD pathogenesis and identify novel biomarkers.

420

421 Employing the bioinformatics tool DAVID and IPA, putative pathway networks were
422 constructed based on the differentially expressed proteins in the BALF proteome that implicated
423 multiple transcription factor pathways and disparate biological processes, such as extracellular
424 space, proteolysis, extracellular matrix, cell adhesion, cytoskeleton, defense response, cell
425 migration, and oxidation-reduction.

426

427 The CANDO platform identified 189 drug candidates that had similar protein interaction
428 signatures based on the BALF proteome when compared to known drugs that are used to treat
429 COPD. However, while most putative drug and protein interactions are likely inhibitors, the

430 induction or inhibition of a target protein is indeterminable with solely the binding potential
431 between drug and protein pairs.

432

433 Topological analysis of the interaction network connecting 233 proteins differentially expressed
434 in COPD through regulatory interactions documented in the literature suggested that ICAM1⁶⁰
435 and galectin-3⁶¹ are important central mediators of inflammation while both fibronectin^{62,63} and
436 vimentin⁶⁴ are central mediators of inflammation and fibrogenesis. This corroborates the results
437 of the pathway enrichment analysis described above, and points to fibrosis and innate
438 inflammation as important processes governing the pathogenesis and progression of COPD. A
439 literature knowledge-based query (Elsevier Knowledge Graph) of drugs with desired drug-target
440 interactions (generated using CANDO) identified putative drugs, such as anti-neoplastic, anti-
441 fibrotic drugs, and regulators of inflammation, that would restore key central proteins to the
442 levels characteristic of healthy controls. Our results also suggest currently utilized medications
443 for COPD have disparate effects on the identified central node proteins that are key putative
444 mediators of COPD pathogenesis and progression. In contrast, the corticosteroid fluocinolone
445 acetonide⁶⁵ and the cardioprotective agent dexrazoxane⁶⁶ were highly enriched for the desired
446 effects on central network entities, both individually and in combination. Fluocinolone acetonide
447 is a stronger potentiator than other corticosteroids of the TGF- β pathway⁶⁷ which is noted to be
448 dysregulated in COPD⁶⁸, and fluocinolone acetonide may be more effective than comparable
449 corticosteroids in improved homeostasis in that pathway. Dexrazoxane⁶⁶ is used to reduce
450 cardiac toxicity associated with anthracycline-based chemotherapy agents by binding to iron and

451 reducing reactive oxygen species; with oxidative stress as a significant factor in COPD

452 pathogenesis⁶⁹, antioxidative therapy may be beneficial.

453

454 The documented actions of these immunomodulators were predicted here to substantially

455 counteract the observed dysregulation of centrally-connected proteins in COPD patients. The

456 relatively high representation of immunomodulators among the candidate agents and the

457 increased centrality of fibrosis-related proteins is consistent with the paradigm of airway

458 remodeling as central to COPD pathology.⁷⁰ With additional data, this regulatory circuit could be

459 used as a testbed for computational evaluation of these and other candidate drug effects using

460 network topological methods.⁷¹

461

462 Limitations and strengths

463 Our approach does has some limitations. The variability in how much BALF is recovered from

464 each aliquot of saline infused in to the lower airway in COPD vs. control subjects are inherent in

465 most BALF proteomic analyses. However, the BALF proteins were normalized to albumin

466 BALF concentrations to account for the variability. The examination of protein levels without

467 accounting for post-translational modifications, such as phosphorylation, may neglect important

468 differences in protein interactions and activity, despite no significant differences in protein

469 levels. Also, the BALF samples were from subjects in the COPD group who were ex-smokers.

470 This exclusion limits the generalizability of our findings particularly current smokers, since the

471 acute effects of tobacco smoke were excluded in our study design.

472

473

474 However, we confined our analysis to ex-smokers with moderate COPD to obtain some
475 uniformity of the COPD phenotype and to avoid the acute inflammatory effects of current
476 smoking. Future work on proteomic profiles will inform us of the difference between such
477 profiles in current smokers and different stages of COPD.

478

479 *Comparison to previously published studies*

480 A sputum proteomics study endeavored to identify COPD severity biomarkers by employing 2D
481 gel electrophoresis and revealed 15 proteins that were significantly differentially expressed
482 between healthy smoker controls and subjects with GOLD stage II; subsequently, 9 of the 15
483 candidate proteins were validated with Western Blot. Of the nine candidate proteins validated
484 with Western Blot, seven were statistically significantly different between groups, specifically
485 albumin, alpha-2-HS glycoprotein, transthyretin, PSP94, apolipoprotein A1, lipocalin-1, and
486 PLUNC.⁷² Employing quantitative ELISA data normalized for protein content, the investigators
487 identified apolipoprotein A1 and lipocalin-1 as statistically differentially expressed in COPD.
488 Although apolipoprotein A1 and lipocalin-1 were identified in our study of the BALF proteome,
489 the proteins were not significantly differentially expressed, likely due to the differences in
490 expression in the different biocompartments of sputum vs. bronchoalveolar lumen.

491 A 2D differential gel electrophoresis study and subsequent mass spectroscopy were performed
492 by Ohlmeier et al., which compared healthy smokers, non-smokers, and smokers with GOLD
493 stage II COPD and revealed a different set of 15 proteins that were differentially expressed
494 between the groups.⁷³ Of these proteins, polymeric immunoglobulin receptor levels in lung tissue
495 and blood between the three groups were correlated with airflow obstruction.

496

497 In Lee et al., tumor-free lung tissue harvested from patients with lung cancer resection, when
498 examined via 2D gel electrophoresis/MALDI-TOF-MS, revealed eight proteins that were
499 upregulated in subjects with COPD compared to nonsmokers and ten significantly differentially
500 expressed proteins between subjects with COPD and smoking subjects without COPD.⁷⁴ Two of
501 the identified proteins, matrix metalloprotease 13 (MMP13) and thioredoxin-like 2, were
502 confirmed to be increased in COPD subjects with Western Blot and immunohistochemical
503 staining, with MMP13 localized to the alveolar macrophage and type II pneumocytes and
504 thioredoxin-like 2 found in the bronchial epithelium. Thioredoxin-like 2, which contains
505 thioredoxin, was found in the BALF proteome but not significantly differentially expressed.
506 However, MMP13 was not identified in our BALF study, likely due to differences in study
507 populations and variable biocompartments.

508

509 **Conclusion**

510 In summary, our work provides a valuable pipeline for identifying many proteins associated
511 with COPD pathogenesis that illustrate the complexity of the development of this disease, as
512 well as identifying putative therapeutic treatment options using cutting-edge bioinformatics
513 approaches. Identifying differentially expressed proteins will form the basis for future
514 mechanistic studies of critical pathways and novel treatment discovery. Validation of our
515 proposed therapeutic approach in animal models and pilot human studies are important next
516 steps.

517

518 **Acknowledgments**

519 The authors like to thank Catherine Wrona for her technical support.

520

521

522

523

REFERENCES

- 524 1. Brown DW, Croft JB, Greenlund KJ, Giles WH. Deaths From Chronic Obstructive Pulmonary
525 Disease-- United States, 2000-2005. *JAMA: Journal of the American Medical Association*.
526 2009;301(13):1331.
- 527 2. From the Global Strategy for the Diagnosis, Management and Prevention of COPD. Global
528 Initiative for Chronic Obstructive Lung Disease (GOLD). Available from:
529 <http://www.goldcopd.org2010>.
- 530 3. Murray CJ, Lopez AD. Mortality by cause for eight regions of the world: Global Burden of Disease
531 Study. *Lancet*. 1997;349(9061):1269-1276.
- 532 4. Kobayashi S, Shibata H, Yokota K, et al. FHL2, UBC9, and PIAS1 are novel estrogen receptor
533 alpha-interacting proteins. *Endocrine research*. 2004;30(4):617-621.
- 534 5. Croft JB, Wheaton AG, Liu Y, et al. Urban-Rural County and State Differences in Chronic
535 Obstructive Pulmonary Disease - United States, 2015. *MMWR Morb Mortal Wkly Rep*.
536 2018;67(7):205-211.
- 537 6. Geitona M, Hatzikou M, Steiropoulos P, Alexopoulos EC, Bouros D. The cost of COPD
538 exacerbations: a university hospital--based study in Greece. *Respir Med*. 2011;105(3):402-409.
- 539 7. Dalal AA, Shah M, D'Souza AO, Rane P. Costs of COPD exacerbations in the emergency
540 department and inpatient setting. *Respiratory Medicine*. 2011;105(3):454-460.
- 541 8. Dalal AA, Christensen L, Liu F, Riedel AA. Direct costs of chronic obstructive pulmonary disease
542 among managed care patients. *Int J Chron Obstruct Pulmon Dis*. 2010;5:341-349.
- 543 9. Dalal AA, Shah M, D'Souza AO, Rane P. Costs of inpatient and emergency department care for
544 chronic obstructive pulmonary disease in an elderly Medicare population. *J Med Econ*.
545 2010;13(4):591-598.
- 546 10. Hutchinson A, Brand C, Irving L, Roberts C, Thompson P, Campbell D. Acute care costs of patients
547 admitted for management of chronic obstructive pulmonary disease exacerbations: contribution
548 of disease severity, infection and chronic heart failure. *Intern Med J*. 2010;40(5):364-371.
- 549 11. Ciapponi A, Alison L, Agustina M, Demian G, Silvana C, Edgardo S. The epidemiology and burden
550 of COPD in Latin America and the Caribbean: systematic review and meta-analysis. *COPD*.
551 2014;11(3):339-350.
- 552 12. Rennard SI, Vestbo J. COPD: the dangerous underestimate of 15%. *Lancet*.
553 2006;367(9518):1216-1219.
- 554 13. Rennard SI, Vestbo J. Natural histories of chronic obstructive pulmonary disease. *Proc Am
555 Thorac Soc*. 2008;5(9):878-883.
- 556 14. Schubert C. Anti-tobacco efforts going up in smoke. *Nat Med*. 2006;12(8):866-866.
- 557 15. Mammen MJ, Sethi S. COPD and the microbiome. *Respirology*. 2016;21(4):590-599.
- 558 16. Rutgers SR, Postma DS, ten Hacken NH, et al. Ongoing airway inflammation in patients with
559 COPD who do not currently smoke. *Thorax*. 2000;55(1):12-18.
- 560 17. Hogg JC. Pathophysiology of airflow limitation in chronic obstructive pulmonary disease. *Lancet*.
561 2004;364(9435):709-721.
- 562 18. Hogg JC, Chu F, Utokaparch S, et al. The nature of small-airway obstruction in chronic
563 obstructive pulmonary disease. *N Engl J Med*. 2004;350(26):2645-2653.
- 564 19. Cosio MG, Saetta M, Agusti A. Immunologic aspects of chronic obstructive pulmonary disease. *N
565 Engl J Med*. 2009;360(23):2445-2454.
- 566 20. Sethi S. Infection as a comorbidity of COPD. *Eur Respir J*. 2010;35(6):1209-1215.
- 567 21. Tu C, Mammen MJ, Li J, et al. Large-scale, ion-current-based proteomics investigation of

568 bronchoalveolar lavage fluid in chronic obstructive pulmonary disease patients. *J Proteome Res.*
569 2014;13(2):627-639.

570 22. Berenson CS, Garlipp MA, Grove LJ, Maloney J, Sethi S. Impaired phagocytosis of nontypeable
571 *Haemophilus influenzae* by human alveolar macrophages in chronic obstructive pulmonary
572 disease. *J Infect Dis.* 2006;194(10):1375-1384.

573 23. Singh D, Agusti A, Anzueto A, et al. Global strategy for the diagnosis, management, and
574 prevention of chronic obstructive lung disease: the GOLD science committee report 2019. *Eur.*
575 *Resp. J.* 2019;53(5).

576 24. Berenson CS, Wrona CT, Grove LJ, et al. Impaired alveolar macrophage response to *Haemophilus*
577 antigens in chronic obstructive lung disease. *Am J Respir Crit Care Med.* 2006;174(1):31-40.

578 25. Tu C, Mammen MJ, Li J, et al. Large-Scale, Ion-Current-Based Proteomics Investigation of
579 Bronchoalveolar Lavage Fluid in Chronic Obstructive Pulmonary Disease Patients. *Journal of*
580 *Proteome Research.* 2014;13(2):627-639.

581 26. Tu C, Li J, Young R, et al. Combinatorial peptide ligand library treatment followed by a dual-
582 enzyme, dual-activation approach on a nanoflow liquid chromatography/orbitrap/electron
583 transfer dissociation system for comprehensive analysis of swine plasma proteome. *Analytical*
584 *chemistry.* 2011;83(12):4802-4813.

585 27. Tu C, Li J, Bu Y, Hangauer D, Qu J. An ion-current-based, comprehensive and reproducible
586 proteomic strategy for comparative characterization of the cellular responses to novel anti-
587 cancer agents in a prostate cell model. *Journal of proteomics.* 2012;7:187-201.

588 28. Huang da W, Sherman BT, Lempicki RA. Systematic and integrative analysis of large gene lists
589 using DAVID bioinformatics resources. *Nat Protoc.* 2009;4(1):44-57.

590 29. Huang da W, Sherman BT, Lempicki RA. Bioinformatics enrichment tools: paths toward the
591 comprehensive functional analysis of large gene lists. *Nucleic acids research.* 2009;37(1):1-13.

592 30. Novichkova S, Egorov S, Daraselia N. MedScan, a natural language processing engine for
593 MEDLINE abstracts. *Bioinformatics.* 2003;19(13):1699-1706.

594 31. Kamdar MR, Stanley CE, Carroll M, et al. Text snippets to corroborate medical relations: an
595 unsupervised approach using a knowledge graph and embeddings. *AMIA Summits on*
596 *Translational Science Proceedings.* 2020;2020:288.

597 32. Cheadle C, Cao H, Kalinin A, Hodgkinson J. Advanced literature analysis in a Big Data world. *Ann*
598 *N Y Acad Sci.* 2017;1387(1):25-33.

599 33. Falls Z, Mangione W, Schuler J, Samudrala R. Exploration of interaction scoring criteria in the
600 CANDO platform. *BMC research notes.* 2019;12(1):318.

601 34. Schuler J, Samudrala R. Fingerprinting CANDO: Increased Accuracy with Structure- and Ligand-
602 Based Shotgun Drug Repurposing. *ACS Omega.* 2019;4(17):17393-17403.

603 35. Mangione W, Falls Z, Chopra G, Samudrala R. cando.py: Open Source Software for Predictive
604 Bioanalytics of Large Scale Drug-Protein-Disease Data. *J Chem Inf Model.* 2020;60(9):4131-4136.

605 36. Hudson ML, Samudrala R. Multiscale Virtual Screening Optimization for Shotgun Drug
606 Repurposing Using the CANDO Platform. *Molecules.* 2021;26(9).

607 37. Schuler J, Falls Z, Mangione W, Hudson ML, Bruggemann L, Samudrala R. Evaluating the
608 performance of drug-repurposing technologies. *Drug Discov Today.* 2021.

609 38. Horst JA, Pieper U, Sali A, et al. Strategic protein target analysis for developing drugs to stop
610 dental caries. *Adv Dent Res.* 2012;24(2):86-93.

611 39. Minie M, Chopra G, Sethi G, et al. CANDO and the infinite drug discovery frontier. *Drug Discov*
612 *Today.* 2014;19(9):1353-1363.

613 40. Sethi G, Chopra G, Samudrala R. Multiscale modelling of relationships between protein classes
614 and drug behavior across all diseases using the CANDO platform. *Mini Rev Med Chem.*
615 2015;15(8):705-717.

616 41. Yang J, Yan R, Roy A, Xu D, Poisson J, Zhang Y. The I-TASSER Suite: protein structure and function
617 prediction. *Nature methods*. 2015;12(1):7-8.

618 42. Yang J, Zhang Y. I-TASSER server: new development for protein structure and function
619 predictions. *Nucleic acids research*. 2015;43(W1):W174-181.

620 43. Yang J, Roy A, Zhang Y. Protein-ligand binding site recognition using complementary binding-
621 specific substructure comparison and sequence profile alignment. *Bioinformatics*.
622 2013;29(20):2588-2595.

623 44. Dutta S, Burkhardt K, Young J, et al. Data deposition and annotation at the worldwide protein
624 data bank. *Mol Biotechnol*. 2009;42(1):1-13.

625 45. Gore S, Sanz Garcia E, Hendrickx PMS, et al. Validation of Structures in the Protein Data Bank.
626 *Structure*. 2017;25(12):1916-1927.

627 46. Dice LR. Measures of the Amount of Ecologic Association Between Species. *Ecology*.
628 1945;26(3):297-302.

629 47. Brands U. A faster algorithm for betweenness centrality [J]. *Journal of Mathematical Sociology*.
630 2001;25(2):163-177.

631 48. Gyorgy A. A Practical Step-by-Step Guide for Quantifying Retroactivity in Gene Networks.
632 *Synthetic Gene Circuits*: Springer; 2021:293-311.

633 49. Team RC. R: A language and environment for statistical computing. 2013.

634 50. Thada V, Jaglan V. Comparison of jaccard, dice, cosine similarity coefficient to find best fitness
635 value for web retrieved documents using genetic algorithm. *International Journal of Innovations
636 in Engineering and Technology*. 2013;2(4):202-205.

637 51. Shapiro SD. Proteolysis in the lung. *The European respiratory journal. Supplement*. 2003;44(44
638 suppl):30s-32s.

639 52. Annoni R, Lancas T, Yukimatsu Tanigawa R, et al. Extracellular matrix composition in COPD. *Eur
640 Respir J*. 2012;40(6):1362-1373.

641 53. Riise GC, Larsson S, Lofdahl CG, Andersson BA. Circulating cell adhesion molecules in bronchial
642 lavage and serum in COPD patients with chronic bronchitis. *Eur Respir J*. 1994;7(9):1673-1677.

643 54. Yang M, Kohler M, Heyder T, et al. Proteomic profiling of lung immune cells reveals
644 dysregulation of phagocytotic pathways in female-dominated molecular COPD phenotype.
645 *Respir Res*. 2018;19(1):39.

646 55. Sethi S. Bacterial infection and the pathogenesis of COPD. *Chest*. 2000;117(5 Suppl 1):286S-
647 291S.

648 56. Stockley RA. Neutrophils and the pathogenesis of COPD. *Chest*. 2002;121(5 Suppl):151S-155S.

649 57. Davies JC, Moskowitz SM, Brown C, et al. VX-659-tezacaftor-ivacaftor in patients with cystic
650 fibrosis and one or two Phe508del alleles. *New england journal of medicine*. 2018;379(17):1599-
651 1611.

652 58. Frick MH, Elo O, Haapa K, et al. Helsinki Heart Study: primary-prevention trial with gemfibrozil in
653 middle-aged men with dyslipidemia. *New England Journal of Medicine*. 1987;317(20):1237-
654 1245.

655 59. Eckland D, Danhof M. Clinical pharmacokinetics of pioglitazone. *Experimental and clinical
656 endocrinology & diabetes*. 2000;108(Sup. 2):234-242.

657 60. Walter RE, Wilk JB, Larson MG, et al. Systemic inflammation and COPD: the Framingham Heart
658 Study. *Chest*. 2008;133(1):19-25.

659 61. Mammen MJ, Sands MF, Abou-Jaoude E, et al. Role of Galectin-3 in the pathophysiology
660 underlying allergic lung inflammation in a tissue inhibitor of metalloproteinases 1 knockout
661 model of murine asthma. *Immunology*. 2018;153(3):387-396.

662 62. Muro AF, Moretti FA, Moore BB, et al. An essential role for fibronectin extra type III domain A in
663 pulmonary fibrosis. *Am J Respir Crit Care Med*. 2008;177(6):638-645.

664 63. To WS, Midwood KS. Plasma and cellular fibronectin: distinct and independent functions during
665 tissue repair. *Fibrogenesis & tissue repair*. 2011;4(1):21.

666 64. Li FJ, Surolia R, Li H, et al. Autoimmunity to vimentin is associated with outcomes of patients
667 with idiopathic pulmonary fibrosis. *The Journal of Immunology*. 2017;199(5):1596-1605.

668 65. Mills J, Bowers A, Djerassi C, Ringold H. Steroids. CXXXVII. 1 Synthesis of a New Class of Potent
669 Cortical Hormones. 6 α , 9 α -Difluoro-16 α -hydroxyprednisolone and its Acetonide. *Journal of the*
670 *American Chemical Society*. 1960;82(13):3399-3404.

671 66. Wiseman LR, Spencer CM. Dexrazoxane. A review of its use as a cardioprotective agent in
672 patients receiving anthracycline-based chemotherapy. *Drugs*. 1998;56(3):385-403.

673 67. Hara ES, Ono M, Pham HT, et al. Fluocinolone acetonide is a potent synergistic factor of TGF- β 3-
674 associated chondrogenesis of bone marrow-derived mesenchymal stem cells for articular
675 surface regeneration. *Journal of Bone and Mineral Research*. 2015;30(9):1585-1596.

676 68. Di Stefano A, Sangiorgi C, Gnemmi I, et al. TGF-beta Signaling Pathways in Different
677 Compartments of the Lower Airways of Patients With Stable COPD. *Chest*. 2018;153(4):851-862.

678 69. Kirkham PA, Barnes PJ. Oxidative stress in COPD. *Chest*. 2013;144(1):266-273.

679 70. Moisieieva NV, Burya LV, Kapustianskaya AA, Kolenko IA, Rumyantseva MA, Shumeiko OH.
680 Comprehensive patterns of comorbidity: copd and depression. Aspects of treatment. *Wiad Lek*.
681 2018;71(3 pt 1):588-591.

682 71. Morris MC, Richman S, Lyman CA, et al. Hacking the Immune Response to Infection in Chronic
683 Obstructive Pulmonary Disease. Paper presented at: 2020 IEEE 20th International Conference on
684 Bioinformatics and Bioengineering (BIBE)2020.

685 72. Nicholas BL, Skipp P, Barton S, et al. Identification of lipocalin and apolipoprotein A1 as
686 biomarkers of chronic obstructive pulmonary disease. *Am J Respir Crit Care Med*.
687 2010;181(10):1049-1060.

688 73. Ohlmeier S, Mazur W, Linja-aho A, et al. Sputum Proteomics Identifies Elevated PIGR levels in
689 Smokers and Mild-to-Moderate COPD. *Journal of Proteome Research*. 2011;11(2):599-608.

690 74. Lee EJ, In KH, Kim JH, et al. Proteomic analysis in lung tissue of smokers and COPD patients.
691 *Chest*. 2009;135(2):344-352.

692

693

Figure/ Figure Legends.

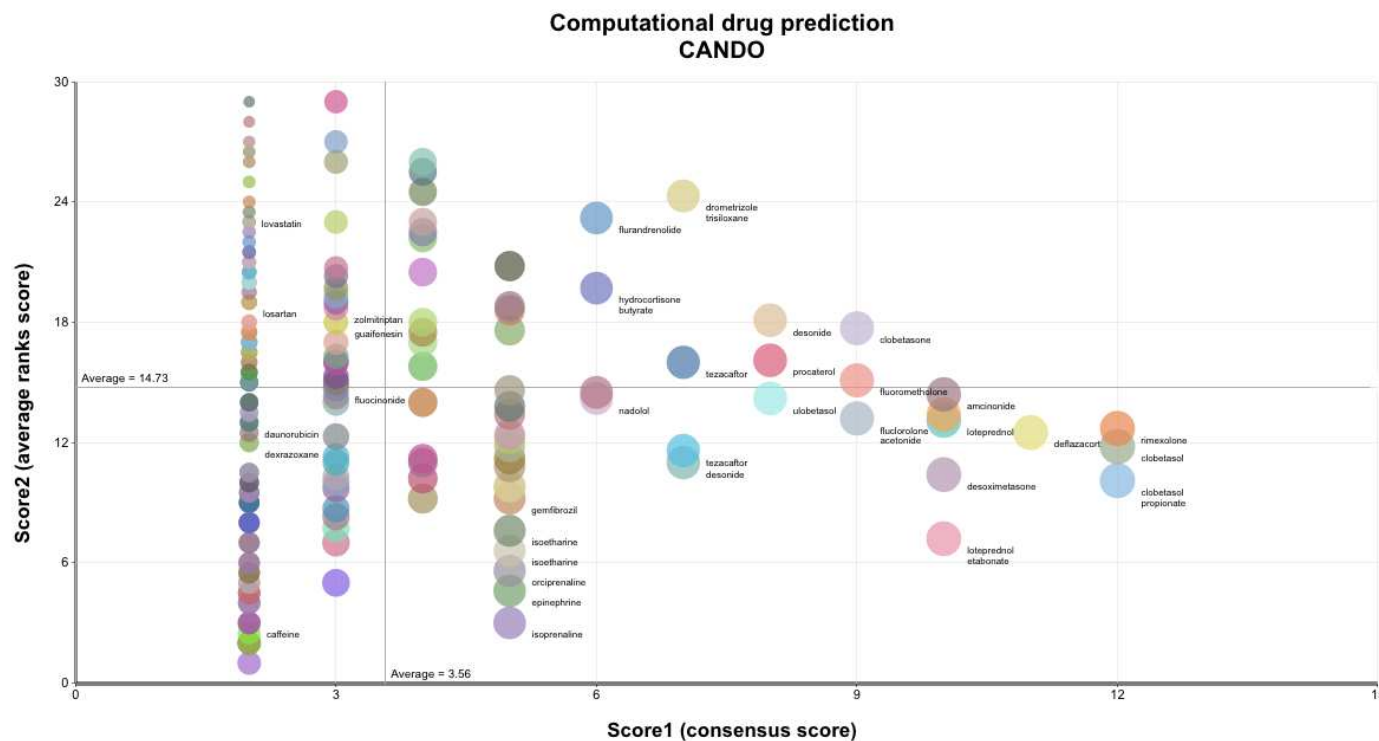


Figure 1 Putative drug candidates for treating COPD generated using the CANDO platform.

A subset of 130 proteins from the CANDO human protein library were identified from 233 differentially expressed proteins in the BALF. These 130 proteins were utilized to generate BALF-specific interaction signatures for 2,450 FDA-approved drugs via our in-house docking protocol BANDOCK (see methods). These drug-proteome interaction signatures were compared to those of 34 known drugs used to treat COPD to predict 189 most similar putative drug candidates. The 189 drugs are represented by colored circles, with the diameter of the circles decreasing with descending overall rank. Drug name labels are depicted for a selection of the 189 drugs shown by the colored circles. The horizontal axis plots the consensus score count or the number of times the particular drug is listed within the top30 most similar drugs to those known to treat COPD based on interaction signature similarity. The vertical axis plots the average of the cumulative ranks of the consensus scores for the putative drug. The overall rank

of a putative drug is determined by initially sorting the drug by the consensus score, as noted above, and then additional sorting by the average rank. Many of the drug candidates were corticosteroids not used to treat COPD; however other putative drugs included tezacaftor, a drug to potentiate sodium channel activity in the treatment of cystic fibrosis; two additional drugs predicted to treat COPD, gemfibrozil, and pioglitazone, are drugs currently used to treat hyperlipidemia and diabetes, respectively. This analysis indicates that the CANDO platform applied to the BALF proteome is able to generate putative drug candidates for COPD treatment.

BANDOCK= bioanalytical docking

CANDO=computational analysis of novel drug opportunities

COPD=chronic obstructive pulmonary disease.

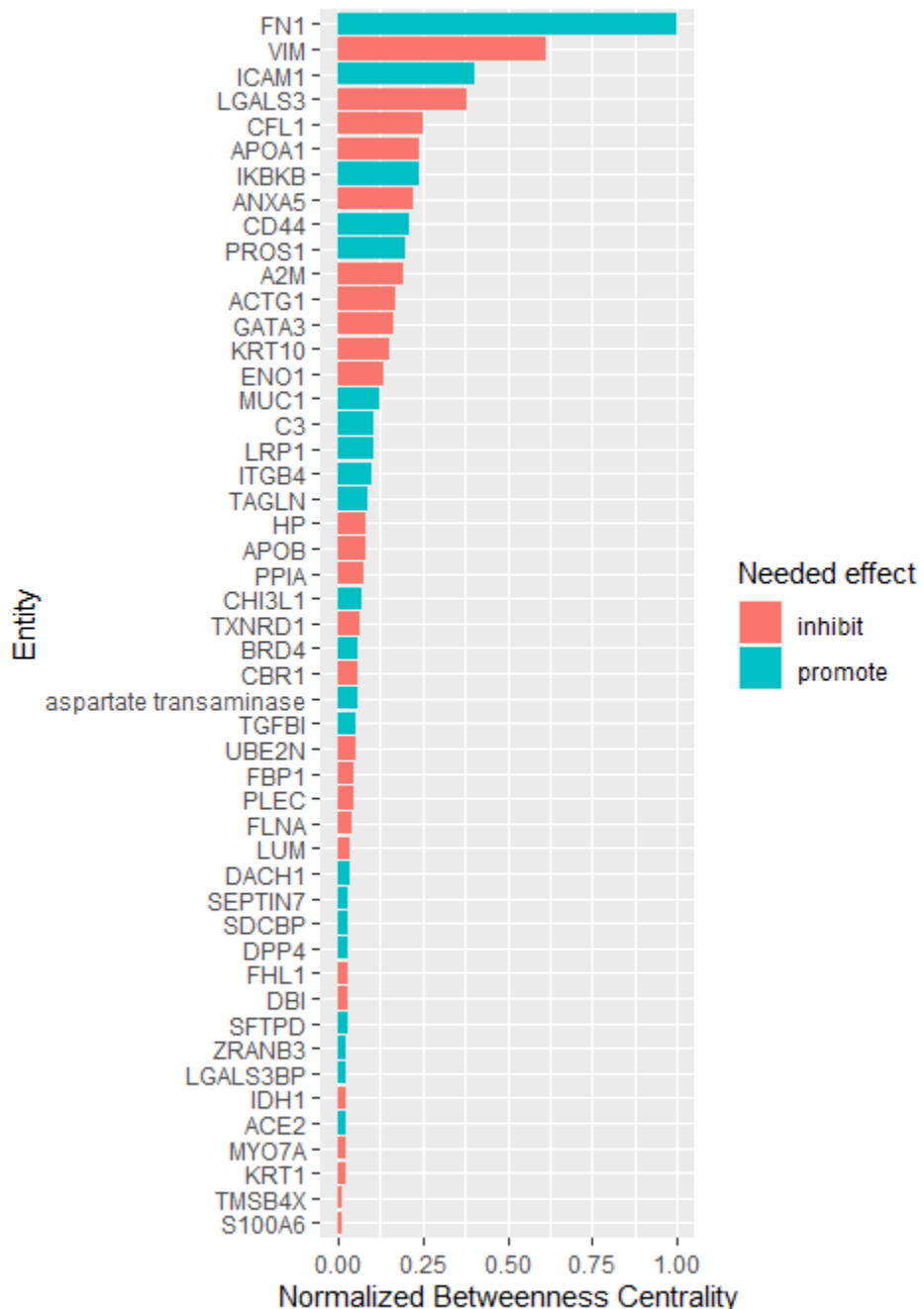


Figure 2 BALF network centrality nodes ranked by betweenness centrality.

Betweenness centrality quantitatively describes how a node (in this case, a differentially expressed protein in the BALF proteome) mediates the interaction between communities of neighboring nodes in the network. Shown are 44 network entities with betweenness centrality >0.01, normalized to the maximum betweenness centrality present in the network. The betweenness centrality scores for all nodes were expressed as fractions of the maximum

betweenness centrality present in the network. The (red and blue) colors indicate the needed effect (inhibition/induction) to restore these entities from COPD levels to the normal levels in healthy control subjects. The four nodes with $\geq 25\%$ of the maximum betweenness centrality (fibronectin) with normalized betweenness centrality values representing a greater than the linear increase from the next lower ranking node are fibronectin, vimentin, intercellular adhesion molecule1 (ICAM1), and galectin-3. These potential key signaling mediators had a betweenness centrality of at least 25% of the maximum. Topological analysis of the interaction network regulatory interactions documented in the literature suggests that these proteins were central mediators of COPD.⁵⁷⁻⁶¹

Colors indicate the needed effect to restore these entities to the normal levels in healthy control subjects.

CANDO=computational analysis of novel drug opportunities

COPD=chronic obstructive pulmonary disease

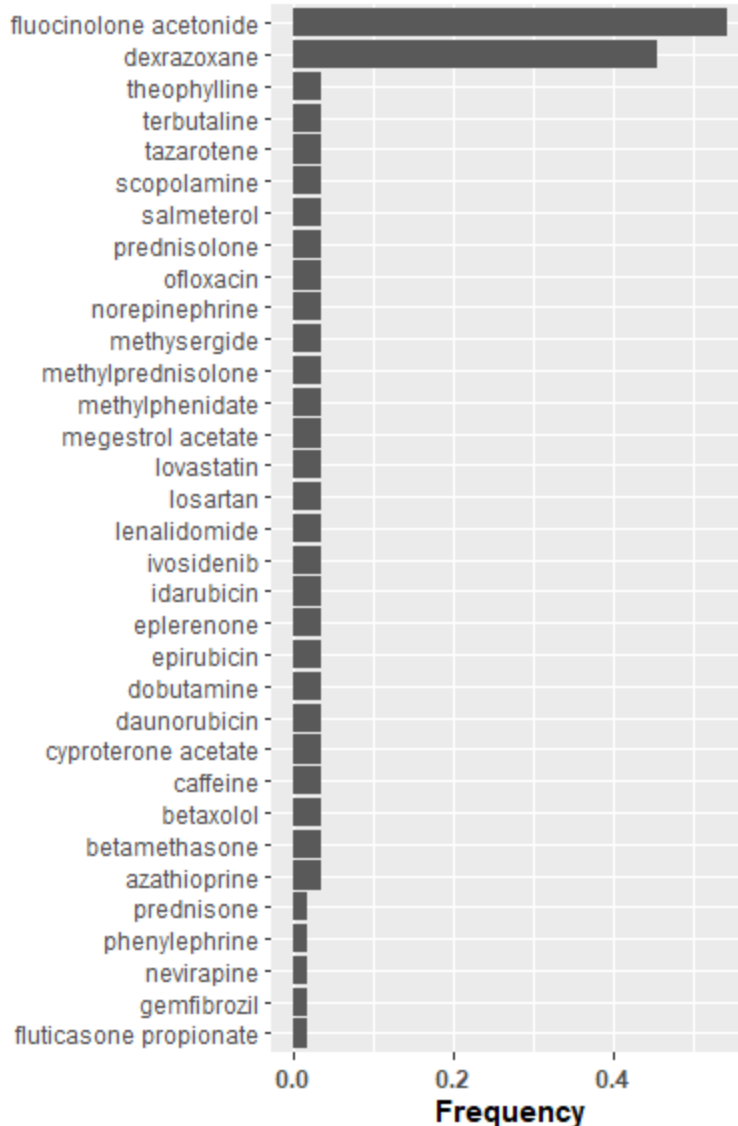


Figure 3. Drug frequency amongst idealized drug combinations predicted to modulate central proteins in COPD. The combinations of drugs initially identified by CANDO, which were predicted to activate or inhibit the four central nodes with the highest maximum betweenness centrality are listed (Figure 2). Drugs that lead to the promotion of central node proteins that were downregulated in the COPD cohort and inhibition of central node proteins (identified by network topological graph) that were overabundant in COPD. The

idealized drug vector constitutes interactions leading to desirable modulation of the central hub protein. Representation of individual drug frequency among the 57 significantly enriched two-drug combinations (idealized drug vectors) out of the 39 proteins represented in the Elsevier Knowledge Graph are listed in descending order. Fluocinolone acetonide and dexamethasone appeared in 54% and 46% of all significantly enriched two-drug combinations respectively, far greater than other drugs appearing in these combinations. The combination of fluocinolone acetonide and dexamethasone is the most enriched two-drug combination leading to an idealized drug vector that most likely reverses the protein levels of the four central nodes to levels found in healthy control subjects.

CANDO=computational analysis of novel drug opportunities

COPD=chronic obstructive pulmonary disease

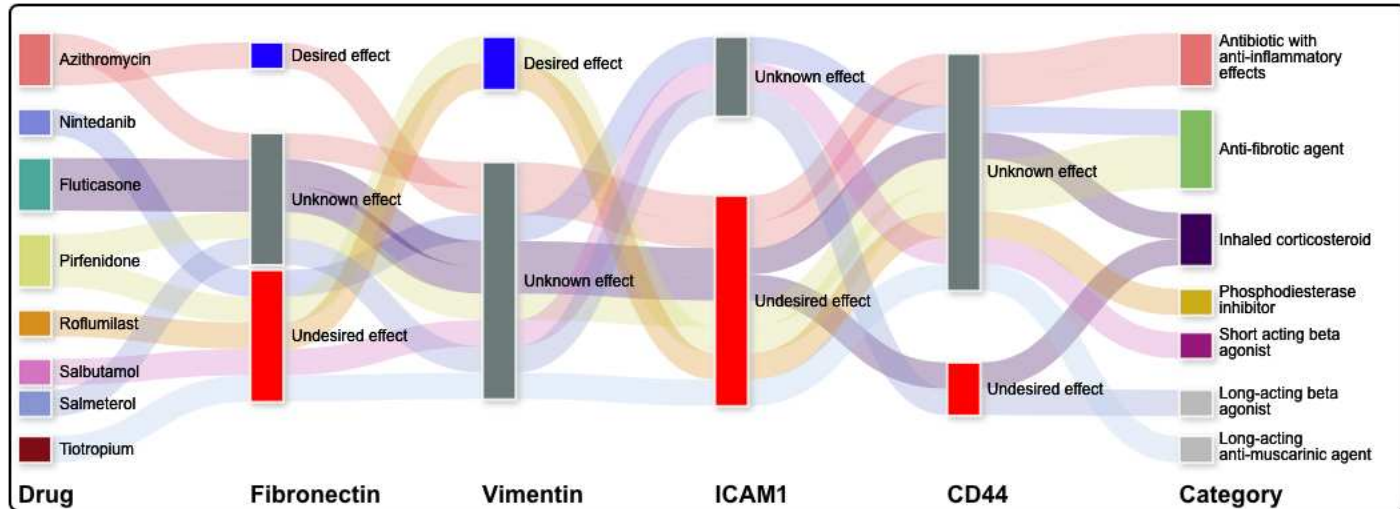


Figure 4: Commonly used pulmonary drugs and their putative effects on four central node proteins in COPD. A Sankey diagram categorizing the likely effects of putative drugs on four central node proteins in COPD is depicted. There are nine drugs on the left of the diagram used to treat different pulmonary diseases, with the corresponding drug classes displayed on the right side of the diagram. The effects of these drugs on four nodes (fibronectin, vimentin, intercellular adhesion molecule1 (ICAM1), and cd44) are detailed in the middle of the diagram, with broad lines connecting the proteins in the right to the putative effect (desired, unknown, undesired). While some of these have been documented to have the desired effect on fibronectin (promotion) or vimentin (inhibition), all have been reported to have the opposite effect on at least one of the most central proteins. This suggests using drugs commonly used to treat pulmonary disease, if repurposed for COPD, may have contrary effects on the mediators of the pathways involved in COPD, reinforcing the need to have a more nuanced approach to drug repurposing.

CANDO=computational analysis of novel drug opportunities

COPD=Chronic obstructive pulmonary disease

TABLES:

Table 1:

Clinical parameters of never-smoking healthy subjects and ex-smokers with stable COPD in BALF study

	Control subjects n=10	COPD subjects (GOLD stage 2) n=10	P-value
Age (years)	63.4 ± 11.7	67.8 ± 8.5	0.15
Sex			0.31
Male	6	7	
Female	4	3	
Race			0.083
Caucasian	8	10	
African-American	2	0	
BMI (kg/m²)	28.5±4.2	32±9.7	0.32
Years patient quit smoking	NA	12.9 ± 4.4	
Tobacco smoking, Pack years	NA	56.6 ± 17.2	<0.001
FEV₁ (% predicted)	96.3 ± 14.8	65.9 ± 8.1	<0.001
FVC (% predicted)	95.6 ± 13.4	87.6± 13.1	0.19
FEV₁/FVC	77.6± 3.8	57.8 ± 8.6	<0.001

Table 1:

Clinical parameters of never-smoking healthy subjects and ex-smokers with stable COPD in BALF study

FEV₁: forced expiratory volume in 1 second. FVC: forced vital capacity. Years quit: Years subjects quit tobacco smoking. Pack-Years: The average number of packs of cigarettes smoked per week multiplied by the years the subject smoked cigarettes.

